Constitutive Activation of Raf-1 Induces Glioma Formation in Mice[1]

Yelena Lyustikman[*,‡,¶], Hiroyuki Momota[#], William Pao[§] and Eric C. Holland[*,†,‡]

*Department of Cancer Biology and Genetics, Memorial Sloan-Kettering Cancer Center, New York, NY 10065, USA; †Departments of Surgery, Neurosurgery, and Neurology, Memorial Sloan-Kettering Cancer Center, New York, NY 10065, USA; ‡Brain Tumor Center, Memorial Sloan-Kettering Cancer Center, New York, NY 10065, USA; §Human Oncology and Pathogenesis Program, Memorial Sloan-Kettering Cancer Center, New York, NY 10065, USA; ¶Graduate Program in Biochemistry, Cell and Molecular Biology, Graduate School of Biomedical Sciences, Weill Medical College of Cornell University, New York, NY 10065, USA; #Neurosurgery Division, National Cancer Center Hospital, 5-1-1 Tsukiji, Chuo-ku, Tokyo 104-0045, Japan

Abstract

In human glioblastoma multiforme (GBM), RAS activity is upregulated in the majority of the tumors. Furthermore, the levels of phospho–mitogen-activated protein kinase/extracellular signal regulated kinase (MAPK/ERK), a downstream effector of RAS, are also increased. In mice, activated KRas cooperates with the loss of *INK4a-ARF* locus or with activated Akt to induce gliomas, confirming an important role for this pathway in glioma biology. However, to correctly target therapies against the RAS signaling pathway, it is necessary to identify the effectors that contribute to RAS-mediated gliomagenesis. In this study, we investigated the contribution of RAF signaling in glioma oncogenesis. We find that the levels of RAF-1 and BRAF proteins and RAF kinase activity are increased in human GBM samples. We confirm the importance of this finding by demonstrating a causal role for a constitutively active Raf-1 mutant in glioma formation in mice. Specifically, we find that activated Raf-1 cooperates with *Arf* loss or Akt activation to generate gliomas similar to activated KRas under the same conditions. Our study suggests that the oncogenic effect of KRas in glioma formation may be transduced at least in part through Raf signaling and that therapeutic targeting of this pathway may be beneficial in glioma treatment.

Neoplasia (2008) 10, 501–510

Introduction

Glioblastoma multiforme (GBM) is a grade IV astrocytoma as defined by the World Health Organization [1]. It is the most common and most malignant type of central nervous system tumor, with a dismal prognosis of about 1 year with extensive resection, chemotherapy, and radiotherapy [2]. One of the reasons this tumor is extremely difficult to treat is its complex biology. Studies of human GBM samples have uncovered a large number of genetic abnormalities. Among those abnormalities, deregulation of signal transduction pathways and loss of cell cycle control are prominent [3].

Disruption of cell cycle control in GBMs commonly occurs through the loss of *INK4a-ARF*, a locus that encodes two proteins, namely,

$p16^{INK4a}$ and $p14^{ARF}$, which in turn control the activity of RB and p53 proteins, respectively. About two-thirds of all human GBMs have lost the *INK4a-ARF* locus [3]. Furthermore, those tumors that do retain the wild-type $p16^{INK4a}$ and $p14^{ARF}$ instead display loss of *p53* and

RB, amplification of *CDK4* and/or *MDM2*, other players involved in cell cycle control [4,5]. Overall, the majority of human GBMs have lost the ability to regulate cell proliferation [3], underscoring the importance of these genetic abnormalities in tumor formation. Causal contribution of *INK4a-ARF* or *p53* loss to gliomagenesis was demonstrated in transgenic mouse models [6–9].

Deregulation of signal transduction pathways is another hallmark feature of most human GBMs. Specifically, overexpression and/or gain-of-function mutations in *EGFR*, *PDGFR*, and *FGFR* receptor tyrosine kinases are frequently observed, leading to the activation of downstream effectors, such as RAS and PI3K/AKT pathways [10]. Activation of AKT is seen in ~70% of GBMs, and increased RAS pathway activity is observed in virtually all GBMs [11–13]. Interestingly, although mutations in *RAS* are frequently observed in other cancer types, they are not found in GBMs, suggesting that increased RAS activity is due to upstream factors [3]. The possible importance of RAS-related signaling to glioma formation is unsurprising, given that RAS is involved in many cellular processes, including proliferation, migration, differentiation, and apoptosis. Indeed, several mouse models of glioma have causally implicated activated HRAS and KRAS in glioma formation [9,14,15]. Extracellular signal–regulated kinase/mitogen-activated protein kinase (ERK/MAPK) signaling, one of the downstream effectors of RAS, is also increased in human GBMs [11,13]. However, whether the oncogenic effect of RAS in gliomagenesis is transduced through the RAF-ERK signaling remains unknown and needs to be addressed to design drugs directed against specific molecular targets. The RAF protein kinases are of particular interest, because they have been shown to be involved in transformation and tumorigenesis [16].

The RAF family of kinases comprises three members: A-, B-, and C-RAF/RAF-1. These serine/threonine kinases have a common structure, with an N-terminal regulatory region and a C-terminal catalytic domain [17]. The best-described downstream effector of RAF is the MEK-MAPK/ERK signaling pathway, although there has been recent speculation about existence of other targets [18]. Mutations in *BRAF* have been observed in melanoma, thyroid, colorectal, and ovarian cancers, among others [19], and recently, germ line mutations associated with a form of leukemia were uncovered in *RAF-1* [20]. However, RAF involvement in gliomagenesis is yet to be studied.

We have previously used the RCAS/tv-a system of gene transfer to somatic cells to show that activated KRas can cooperate with activated Akt or *INK4a-ARF* loss to induce gliomas in mice [21,22]. Here, we sought to determine whether the RAF-MEK-ERK signaling pathway, one of the downstream effector of KRas, is involved in gliomagenesis. In this study, we show that the levels of RAF-1 and BRAF proteins and RAF kinase activity are upregulated in the majority of human GBMs. Furthermore, we used the RCAS/tv-a system to address the gliomagenic ability of a constitutively active Raf-1 mutant [23] in glial progenitors. We show that Raf-1 activation cooperates with *INK4a-ARF* loss or Akt activation in glioma formation in mice. The Raf-1 tumors are very similar to those induced by KRas in incidence and histologic features. These results indicate that RAS contributes to human GBM formation in part through RAF signaling. Our findings reveal potential therapeutic targets important to the biology of GBM.

Materials and Methods

DNA Constructs and DF1 Cell Transfection

RCAS-KRas[G12D], RCAS-Akt, and RCAS-eGFP have been described previously [10]. RCAS-KRas was a gift from Harold Varmus

(Memorial Sloan-Kettering Cancer Center). RCAS-Akt/HA, which carries the activated form of Akt designated Akt-Myr D11-60 and has an HA tag sequence added to the 3′-end of the cDNA, was a gift from Peter Vogt (Scripps Institute, La Jolla, CA). pBABEpuro-ΔRaf1-22W was kindly provided by C.M. Counter (Duke University, Durham, NC). The ΔRaf1-22W fragment was released with an *Eco*RI digest and cloned into pYAP6 cut with *Eco*RI. After confirming the correct orientation, a *Not*I/*Cla*I fragment was released and subcloned into RCAS-Y to generate RCAS-ΔRaf1-22W. DF1 packaging cells were obtained from American Type Culture Collection (ATCC, Manassas, VA) and maintained in ATCC medium (Cat. #30-2002), supplemented with 10% fetal calf serum in a humidified atmosphere at 39°C and 5% CO_2. Transfections with RCAS plasmids were performed as previously described [21].

Generation and Infection of Primary Brain Cultures

Brains of P0 neonatal *Ntv-a wt* mice were isolated and dissociated in DMEM medium supplemented with 10% FBS. Following centrifugation at 1000*g*, cells were resuspended in DMEM/10% FBS, plated on 100-mm tissue culture dishes and maintained in a humidified atmosphere at 37°C and 5% CO_2. Infection with RCAS viruses was performed as described previously [6]. Briefly, conditioned media from ~80% confluent DF1 cells transfected with RCAS plasmids were collected, filtered through 0.22-μm filters (Nalgene, Rochester, NY), and applied to ~40% to 50% confluent *Ntv-a wt* glial progenitors. Infections were repeated four times in 24-hour intervals. RCAS-GFP was used as an infection control in all experiments.

Human Brain Tissue

All human brain tumor samples were obtained from the Memorial Sloan-Kettering Cancer Center tissue bank with the approval of the institutional review board. Normal brain cortex was obtained from adult human autopsy (Analytical Biological Services, Inc., Wilmington, DE). The samples were flash frozen in liquid nitrogen immediately after removal and were stored at –80°C.

Lysate Preparation

Glial progenitors infected with RCAS viruses as above were maintained in serum-free medium overnight, washed three times with ice-cold PBS, harvested, and pelleted. Cold lysis was performed in mammalian protein extraction reagent (M-PER; Pierce, Rockford, IL), supplemented with 100 mM NaCl, 30 mM NaF, 1 mM EDTA, 0.5 mM PMSF, 1 mM Na_3VO_4, and protease inhibitor cocktail (Roche, Indianapolis, IN), and protein concentrations were determined using the Bio-Rad Protein Assay Reagent (Bio-Rad, Hercules, CA).

To prepare human tissue lysates, frozen GBM samples and control normal cortex were ground into powder in liquid nitrogen using a mortar and pestle. Cold lysis was performed using T-Per (Pierce), supplemented with 30 mM NaF, 1 mM Na_3VO_4, 1 mM PMSF, and inhibitor cocktail (Roche), for 45 minutes with rotation. Cleared lysates were measured for protein concentration using the Bio-Rad Protein Assay Reagent (Bio-Rad).

Western Blot Analysis

A total of 100 μg of total protein were resolved on a 10% SDS-PAGE gel and were transferred to polyvinylidene difluoride membrane (Millipore, Bedford, MA). After blocking with 5% nonfat milk

in PBS–0.1% Tween-20 (PBST), membranes were incubated overnight with the following primary antibodies diluted in 5% nonfat milk in PBST (or 5% BSA in PBST for phospho-specific antibodies): anti–phospho-Erk1/2$^{ser217/221}$ (Cell Signaling Technology, Beverly, MA), 1:1000; anti–Erk1/2 (Cell Signaling Technology), 1:1000; anti–Raf-1 (sc-133; Santa Cruz Biotechnology, Santa Cruz, CA), 1:200; anti-Braf (Santa Cruz Biotechnology), 1:200; anti–phospho-Mek1/2 (Cell Signaling Technology), 1:1000; anti–Mek1/2 (Cell Signaling Technology), 1:1000; anti–phospho-Akt^{Ser473} (Cell Signaling Technology), 1:1000; anti-Akt (Cell Signaling Technology), 1:1000; and anti-KRas (Santa Cruz Biotechnology), 1:200. For loading control, incubation for 1 hour with anti-GAPDH (Advanced ImmunoChemical, Long Beach, CA) at 1:1000 or with anti-actin (Santa Cruz Biotechnology) at 1:500 in 5% nonfat milk in PBST was used. Secondary antibodies were diluted 1:1000 in 5% nonfat milk in PBST. Secondary peroxidase–conjugated anti-rabbit (Amersham Biosciences, Piscataway, NJ), anti-goat (Roche), and anti-mouse (Roche) antibodies were used. Signal was developed using an enhanced chemiluminescence kit (Amersham Biosciences) and was visualized on a film (BioMax MR; Kodak, Rochester, NY). To probe for multiple antibodies, membranes were stripped using a stripping buffer (Pierce) according to the manufacturer's instructions. Incubation using the appropriate secondary antibody only followed enhanced chemiluminescence was used to determine the completeness of stripping. Membranes were reblocked in 5% nonfat milk in PBST before the new primary antibodies were applied. For quantification, band density was determined using ImageJ software and was normalized against loading control. Statistical analysis was performed with GraphPad Prism4 software (GraphPad Software Inc., San Diego, CA) using the two-tailed Student's t test. P values $< .05$ were considered significant.

RAF Kinase Assay

Ground frozen GBM samples, normal cortex tissue, and control cell pellets were lysed at 4°C in buffer A [50 mM Tris–HCl pH 7.5, 100 mM NaCl, 1% Triton X-100, 50 mM NaF, 10 mM Na$_3$PO$_4$, 5 mM EDTA, 1 mM Na$_3$VO$_4$, 1 mM PMSF, and inhibitor cocktail (Roche)] for 45 minutes with rotation. Cleared lysates were measured for protein concentration, and 100 µg of total protein was used for the kinase assay. The assay was performed immediately using the Raf kinase activity kit (Cat. #17-357; Upstate Technologies, Lake Placid, NY) according to the manufacturer's instructions. Briefly, lysates containing 100 µg of total protein were incubated with recombinant inactive MEK1, inactive ERK2, and cold ATP. After a 30-minute incubation at 30°C with agitation, 4 µl of the reaction mixture (Step1) was used for the second step of the assay. In this step (Step2), 4 µl of Step1 were incubated for 10 minutes at 30°C with [γ-^{32}P]ATP and recombinant Erk2 substrate myelin basic protein. The Step2 reactions were spotted onto nitrocellulose paper and were washed extensively. ^{32}P incorporation was quantified using a scintillation counter (Perkin-Elmer, Waltham, MA). Astrocytes expressing activated Raf-1 were used as a positive control, and astrocytes expressing eGFP were the negative control. Statistical comparison was performed with GraphPad Prism4 software (GraphPad Software Inc.) using the two-tailed Student's t test. P value $< .05$ was considered significant.

RAL Activity Assay

Ground frozen GBM samples and normal cortex tissue were lysed at 4°C in buffer B (50 mM Tris–HCl pH 7.5, 200 mM NaCl, 1% NP-40, 10 mM MgCl$_2$, and 0.5 mM dithiothreitol). Cleared lysates were measured for protein concentration, and 800 µg of total protein was used for the assay. The levels of activated RAL (RAL-GTP) were measured using GST-RalBP1 agarose beads (Upstate Technologies) according to the manufacturer's instructions. Briefly, the lysates were incubated with the GST-RalBP1 beads for 30 minutes at 4°C with rotation, followed by three washes with buffer B. Proteins were resolved on a 12.5% SDS-PAGE and were processed as above. Membranes were incubated overnight with anti-RalA antibody (BD Transduction Laboratories, San Jose, CA) diluted 1:3000 in 5% nonfat milk in PBST, followed by HRP-conjugated anti-mouse antibody (Roche) 1:1000 in 5% nonfat milk in PBST for 1 hour at room temperature, and developed as above. In addition, 10% of the input lysate was resolved on a 12.5% SDS-PAGE and processed as above to determine the levels of total RalA in the samples.

Generation of Tumor-Bearing Mice

All mouse strains used in this study have been described [6,22]. DF1 cells producing the appropriate RCAS viruses were cultured to ~80% confluence. Approximately 10^4 cells in a 1-µl volume were injected intracranially into the right frontal cortical areas of neonatal (P0 to P1) mice using a Hamilton syringe. Statistical analysis was performed with GraphPad Prism4 software (GraphPad Software Inc.) using the log-rank test applied to Kaplan–Meier graphs.

Brain Sectioning, Hematoxylin and Eosin Staining, and Immunohistochemistry

Tissue processing, sectioning, and hematoxylin and eosin staining were performed as described previously [6]. Primary antibodies were diluted as follows: anti–proliferating cell nuclear antigen (PCNA) (Oncogene Research Products, Cambridge, MA), 1:100; anti–phospho-Erk1/2, anti–phospho-Akt^{S473}, and phospho-S6RP (Cell Signaling Technology), 1:50; anti–glial fibrillary acidic protein (GFAP) (MAB3402; Chemicon, Temecula, CA), 1:1000; anti-nestin (BD Pharmingen, San Jose, CA), 1:200; and anti-p19^{Arf} (Santa Cruz Biotechnology), 1:200. Sections were incubated overnight at 4°C. The appropriate secondary biotinylated antibodes (Vector BioLabs, Philadelphia, PA) were used at 1:250 for 1 hour at room temperature. All antibodies were diluted in 5% horse serum PBS–0.05% Tween-20. Peroxidase signal was developed using the ABC kit (Vector) and visualized using the DAB substrate (Vector). Control stainings using secondary antibody only were performed for all antibodies.

Immunocytochemistry

Cells were seeded on glass coverslips and grown to approximately 50% confluence. After fixation with 4% paraformaldehyde for 20 minutes at room temperature, cells were washed three times with PBS, permeabilized for 10 minutes with PBS/0.5% Triton X-100, washed again once with PBS, and blocked with PBS/3% BSA for 30 minutes. Primary anti–nestin rabbit polyclonal antibody (BD Pharmingen) was applied at 1:500 dilution in PBS/3% BSA overnight at 4°C. Cells were washed three times with PBS and were incubated with Alexa Fluor 555–conjugated anti-rabbit secondary antibody (Molecular Probes, Eugene, OR) at 1:300 in PBS/3% BSA for 1 hour at room temperature. After washing three times with PBS, cells were counterstained with 4′,6-diamidino-2-phenylindole and then washed, and the coverslips were mounted using 70% glycerol.

Results

RAF Activity Is Increased in Human GBMs

Whereas RAS activity and phospho-ERK levels are upregulated in human GBMs, the activity status of the intermediate members of this pathway is unknown. We addressed the status of RAF kinases in these tumors, as they are directly downstream of RAS and are implicated in many cancer types [19]. We analyzed 20 human GBM specimens, as well as 7 oligodendrogliomas. First, we determined the total levels of RAF-1 and BRAF proteins in these tumors and compared them to the normal human brain cortex. The levels of total RAF-1 and BRAF in the majority of the tumors were significantly increased in comparison to normal brain tissue (Figure 1, A and B). We also analyzed the status of AKT and RAL, other effectors known to be downstream of RAS. We found that levels of phosphorylated AKT were upregulated in the majority of the tumors,
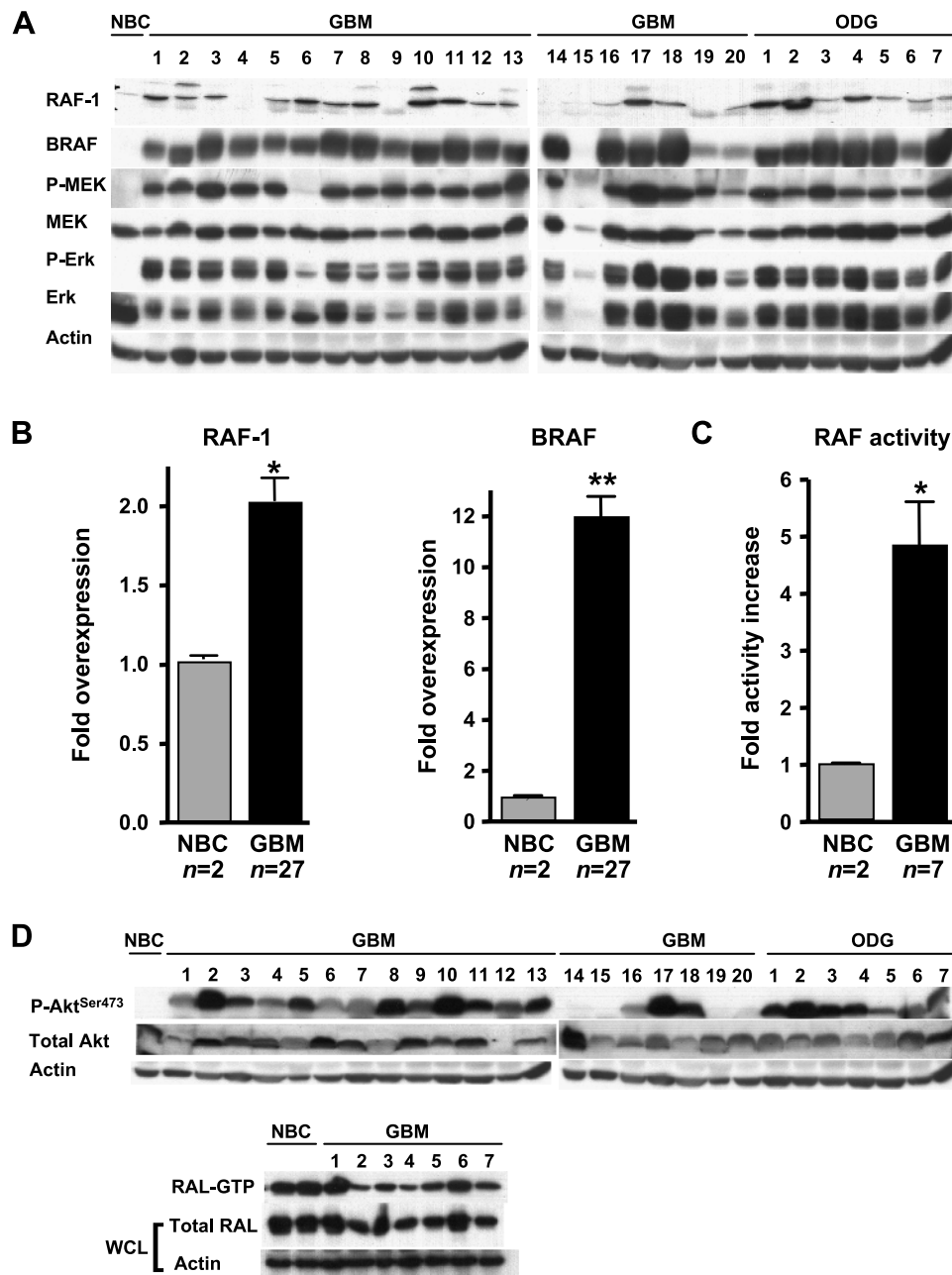
Figure 1. RAF activity is increased in human GBMs. (A) RAF signaling pathway in a group of 20 human GBM specimens and 7 human oligodendrogliomas compared to normal brain cortex (NBC). Actin was used as a loading control. (B) Quantification of RAF protein levels in (A), *$P < .05$, **$P < .01$. (C) Total RAF kinase activity in a subset of the GBMs ($n = 7$) examined in (A). Normal brain cortex ($n = 2$) was used as a negative control. C32 cell line, which has the activating V600E mutation in *BRAF*, was used as a positive control. The graph represents the mean ± SD (bars) of at least three independent experiments. *$P < .05$. (D) Analysis of AKT and RAL activities in human tumors. Western blot analysis of 20 GBM and 7 oligodendroglioma (ODG) samples shows increased Ser473 phosphorylation of AKT compared to NBC. Levels of GTP-bound (active) RAL in 7 GBM specimens show a slight decrease in activity compared to two normal cortex samples (NBC). Levels of total RAL protein were examined using 10% of the input whole-cell lysate (WCL). Actin was used as a loading control.
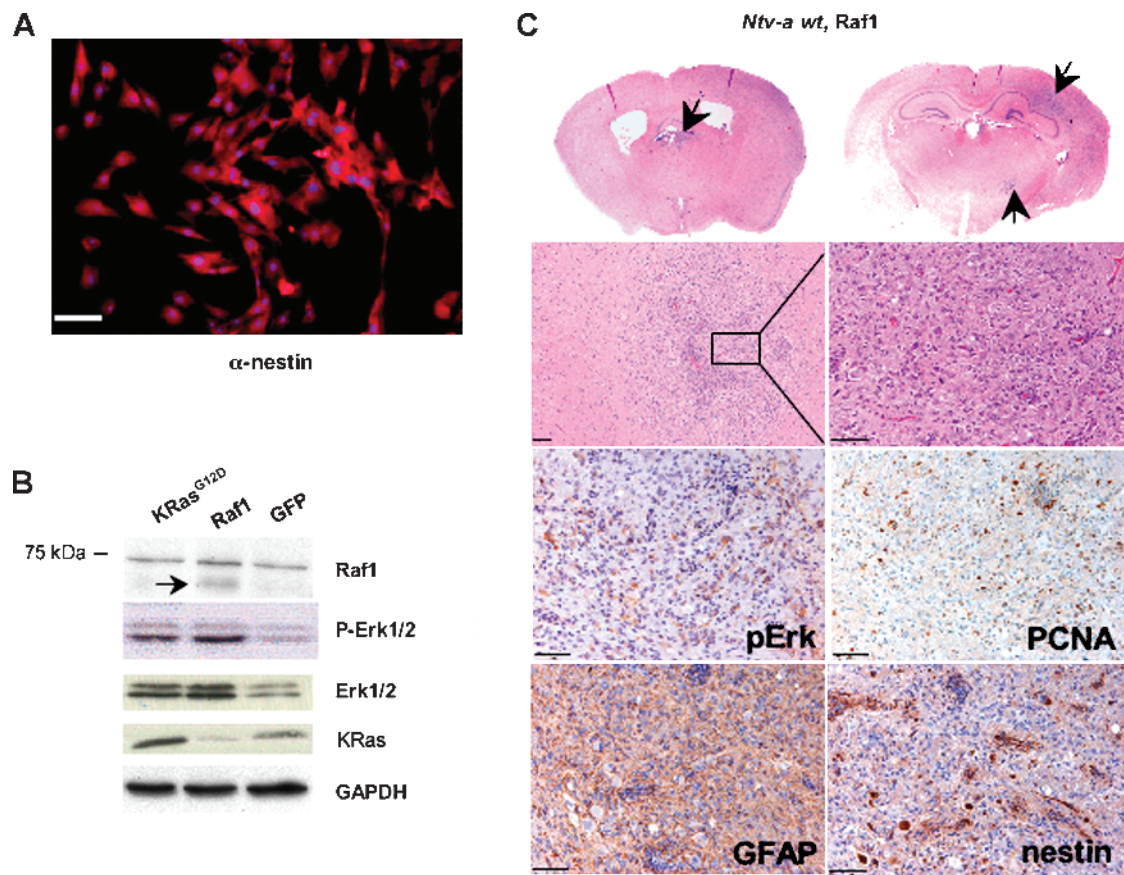
Figure 2. RCAS-Raf1 induces small hyperplastic lesions in *Ntv-a wt* mice. (A) Glial progenitors were isolated from newborn mouse pups (P0) and grown in culture as described in the Materials and Methods section. Progenitor status was confirmed by immunofluorescence staining against nestin (nestin in red and DAPI staining in blue); scale bar, 50 μm. (B) Activities of the viral *KRas* and *Raf-1* mutants were confirmed by infecting primary *Ntv-a* glial progenitors with the appropriate RCAS viruses and assaying for Raf-1, phospho-Erk1/2 and total Erk1/2, and KRas levels. Mutant Raf-1 is indicated with an arrow; molecular size marker is shown to the left. RCAS-GFP was used as an infection control. GAPDH was used as a loading control. (C) Representative examples of small lesions induced in *Ntv-a wt* mice. An hematoxylin and eosin staining illustrates the morphology of a typical *Ntv-a wt* lesion (original magnifications of second row: left panel, ×100 and right panel, ×200). Immunohistochemical analysis indicates Erk activation, whereas GFAP and nestin stainings suggest glial character. Proliferation is evidenced by PCNA-positive cells. Scale bar, 50 μm.

underscoring the importance of this pathway in glioma biology [10], whereas levels of activated RAL (RAL-GTP) were slightly downregulated (Figure 1*D*). To confirm that our findings were not simply due to the high proliferation rate of the tumors compared to normal tissue, we compared primary mouse astrocytes synchronized in G_0 by serum starvation to the normally replicating astrocytes. Western blot analysis showed no differences in either B-Raf or Raf-1 between the two treatments (data not shown). However, the levels of phospho-Erk increased slightly in replicating cells, indicating that this signaling cascade may be regulated in part by the cell cycle status (data not shown). Next, we measured RAF kinase activity to find whether it correlated with the increased protein levels. In analyzing 7 GBM samples (from the above pool of 20), we saw that, although the RAF kinase activity levels varied between specimens, they were consistently significantly higher compared to normal tissue (Figure 1*C*). This suggested that the overexpessed RAF kinases were active. The increased kinase activity was due neither to the commonly observed BRAF V600E mutation [19] nor to any activating RAF-1 mutations as determined by DNA sequencing (data not shown). These data are in line with a recent report that analyzed a total of 93 gliomas of various histologic subtypes and found only two cases of mutation of *BRAF*, whereas gene copy am-

plification was present in nearly 50% of the tumors analyzed [24]. Of note, *EGFR* gene amplification was also frequently seen in the tumors with amplified *BRAF* [24]. Both *BRAF* and *EGFR* genes are located on chromosome 7 (7q34 and 7p12, respectively), making their coamplification possible when the entire chromosome 7 is gained. Additionally, array comparative genomic hybridization analysis of 87 GBMs did not detect gene amplification of *RAF-1* (Cameron Brennan, personal communication). Although the exact mechanisms of overexpression are unknown, it may be mediated by upstream effectors such as activated RAS and growth factor receptors, which are known to be activated in these tumors [11,12,25]; increased expression of the RAF proteins provided a selective advantage to accommodate increased signaling through these pathways. Overall, the results of the human tumor analysis suggested the importance of this signaling pathway and prompted us to address its possible causal role in glioma formation.

### Constitutive Activation of Raf-1 Induces Hyperplastic Lesions in *Ntv-a* Mice

The RCAS/tv-a system of gene transfer to somatic cells has been described [26]. We have previously used this system to demonstrate a causal role for KRas activation in gliomagenesis. Specifically, we

showed that constitutively active KRas can cooperate with a loss of *INK4a-ARF* to induce spindle-cell gliomas [8,22] or with activated Akt to induce GBMs [10,13,21]. Here, we sought to determine whether activation of Raf-1, one of the downstream effectors of KRas, similarly contributes to gliomagenesis. In human gliomas, both RAS and RAF are wild-type, and continuous signaling is mediated by up-regulation of upstream effectors such as hyperactive epidermal growth factor receptor (EGFR). In the absence of signaling by these regulators in our system, we instead used a constitutively active mutant of Raf-1, ΔRaf1-22W, previously shown to transform NIH 3T3 cells *in vitro* [23] and studied its tumorigenic ability compared to the activated KRas mutant.

We first tested ΔRaf1-22W *in vitro* to ensure that it was active in glial progenitors. We generated primary cell cultures derived from brains of neonatal (P0) *Ntv-a* mice. These cultures consisted 100% of tv-a–expressing glial progenitors as confirmed by immunofluorescence staining for the neural progenitor marker nestin (Figure 2*A*). We next infected these cultures with RCAS-ΔRaf1-22W (hereafter referred to as RCAS-Raf1), RCAS-KRas^{G12D}, or RCAS-GFP as a control. RCAS-Raf1 and RCAS-KRas^{G12D} induced phosphorylation of Erk1/2 to similar levels (Figure 2*B*), indicating that both con-

structs were active. Interestingly, increased levels of total Erk1/2 were seen in both RCAS-KRas^{G12D}– and RCAS-Raf1–infected cells compared to RCAS-GFP controls, suggesting the presence of positive feedback during the activation of this pathway [27].

Next, we looked at the tumorigenic ability of RCAS-Raf1. We injected neonatal *Ntv-a wt* mice with DF1 cells producing RCAS-Raf1 or RCAS-KRas^{G12D} (*n* = 30 for each construct). Animals were monitored for symptoms of glioma formation such as lethargy, poor grooming, weight loss, and hydrocephalus. None of the animals injected with either RCAS construct became moribund due to glioma formation during the duration of the experiment. Therefore, all animals were sacrificed at the 14-week endpoint, and their brains were analyzed for the presence of any asymptomatic lesions. Whereas none of the wild-type mice injected with RCAS-KRas^{G12D} showed any brain abnormalities, in line with our previous data, approximately 30% of the mice injected with RCAS-Raf1 displayed small hyperplastic lesions in the cortex (Figure 2*C*). These lesions were glial in character, as indicated by GFAP immunostaining. Furthermore, increased phospho-Erk immunostaining suggested activation of KRas signaling, and PCNA staining indicated that the lesions were proliferating (Figure 2*C*). However, the lesions did not progress to fully developed gliomas, confirming that
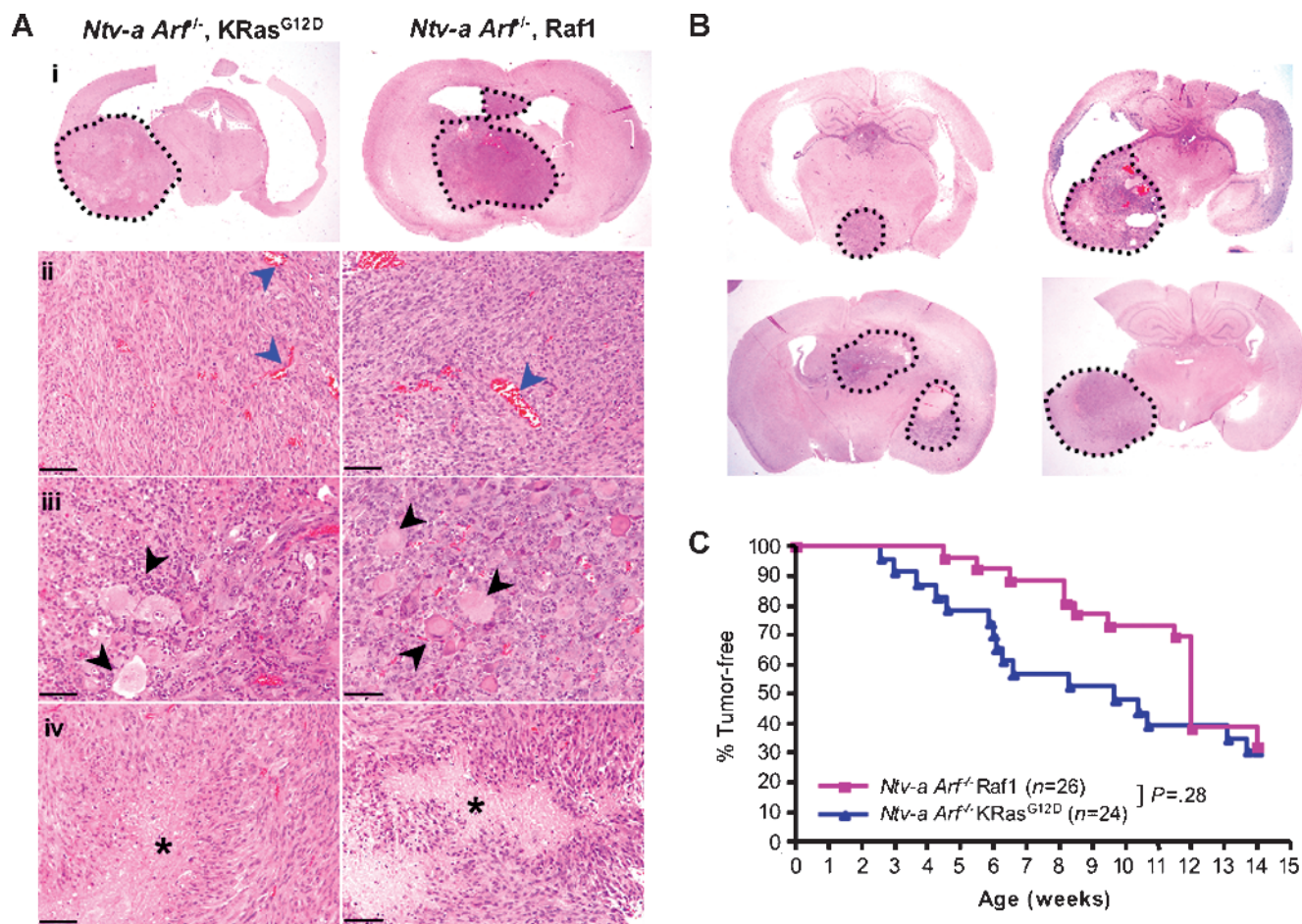
Figure 3. Raf-1 activation induces gliomas in *Ntv-a;Arf*$^{-/-}$ mice. (A) A representative KRas-induced glioma (*i*, left) and Raf-1–induced glioma (*i*, right) in *Ntv-a;Arf*$^{-/-}$ background. A higher magnification reveals spindle-cell sarcoma-like morphology, with microvascular proliferation (*ii*, microvasculature indicated with blue arrowheads), giant cells (*iii*, black arrowheads), and pseudopalisading necrosis (*iv*, asterisk). Scale bar, 50 μm. (B) Examples of gliomas induced with RCAS-Raf1 in different parts of the brain in *Ntv-a;Arf*$^{-/-}$ background. (C) Kaplan–Meier analysis comparing KRas- and Raf-1–induced tumors in *Ntv-a;Arf*$^{-/-}$ mice. *P* = .28 (ns).
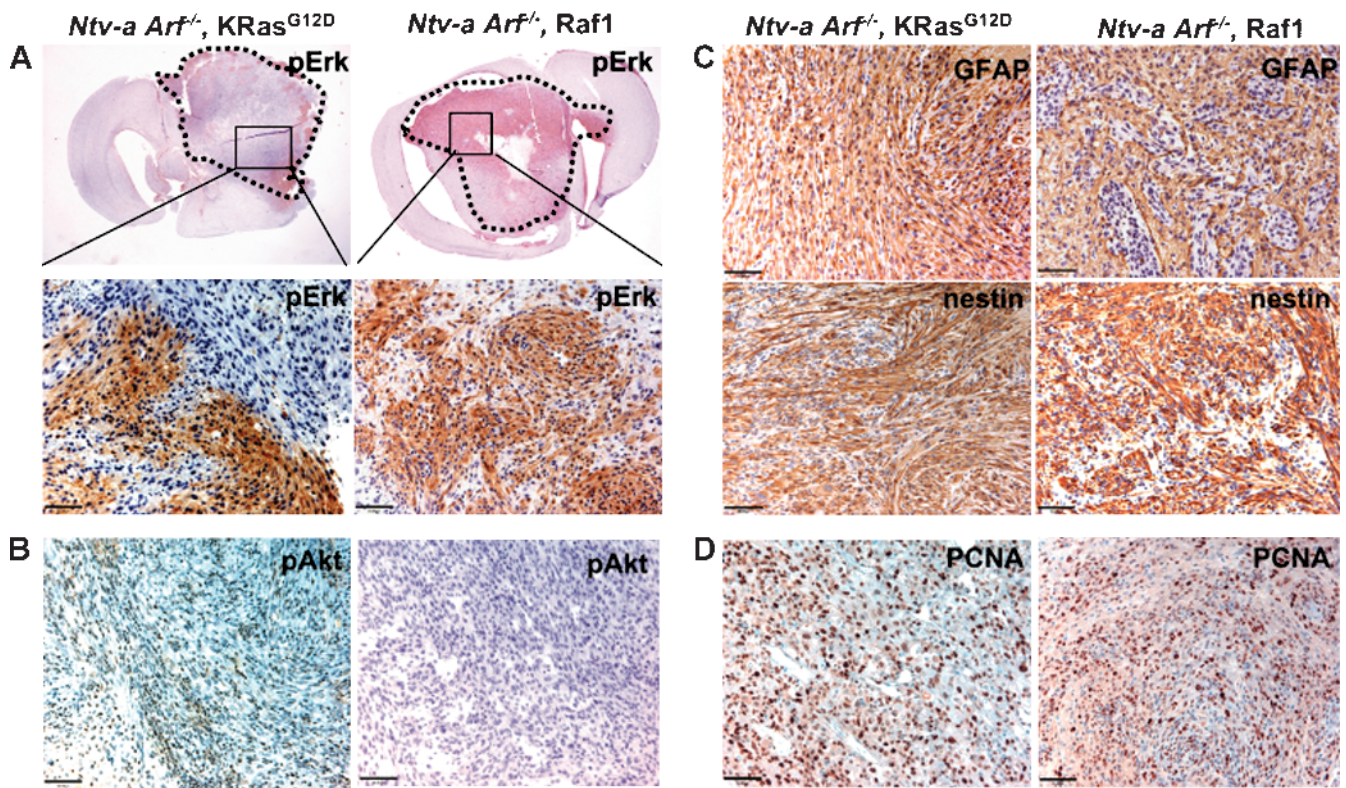
Figure 4. Immunohistochemical comparison of KRas- and Raf-1–induced tumors in *Ntv-a;Arf* $^{-/-}$ mice. Representative immunohistochemical patterns of each tumor type are illustrated. Note patchy phospho-Erk staining in KRas glioma *versus* a more homogeneous staining pattern in Raf-1 glioma (A); scale bar, 50 μm.

activation of MAPK signaling alone is insufficient for glioma formation. To study the possibility that the 14-week time period was not long enough to allow these lesions to progress further, we extended the experiment to 6 months for a subset of *Ntv-a wt* RCAS-Raf1–injected animals but did not observe additional tumor progression (data not shown). We also explored the possible loss of p19^{Arf} as a contributing factor in the formation of the lesions. Immunohistochemical staining for p19^{Arf} showed presence of Arf-positive cells (data not shown), suggesting that *Arf* loss was likely not the causal event during initiation of lesion formation.

Raf-1 Activation Cooperates With Arf Loss in Glioma Formation

To investigate whether KRas^{G12D} and Raf-1 are similarly able to cooperate with *Arf* loss to induce gliomas, we injected *Ntv-a;Arf* $^{-/-}$ animals with RCAS-KRas^{G12D}– or RCAS-Raf1–producing DF1 cells (*n* = 24 and 26, respectively). As discussed earlier, RCAS-KRas^{G12D}– induced high-grade gliomas in *Ntv-a;Arf* $^{-/-}$ mice, with spindle-cell morphology, occasional pseudopalisading necrosis, and extensive microvascular proliferation (Figure 3A). Similarly, RCAS-Raf1 induced high-grade gliomas in *Ntv-a;Arf* $^{-/-}$ animals, with histologic features similar to KRas-induced tumors (Figure 3, A and B). In particular, both tumor types were polymorphic, with the presence of spindle cells and cells with more astrocytic character, with a considerable overlap of features. They were both characterized by large numbers of giant cells, occasional presence of gemistocytes, fascicular cell growth, and endothelial proliferation. The overall incidence of glio-

mas induced with KRas and Raf-1 was also similar, 69.6% and 65.4%, respectively, although the tumor latency was somewhat shorter in KRas tumors (Figure 3C). The increased latency in Raf-1 tumors could be due to the fact that KRas has other known downstream effects in addition to the Raf-Erk signaling cascade that could enhance tumor initiation [28] or because of different levels of expression of RCAS-KRas^{G12D} and RCAS-Raf1.

We also compared the immunohistochemical characteristics of KRas and Raf-1 gliomas by analyzing 10 tumors of each type. Interestingly, although both KRas and Raf-1 tumors stained highly for phospho-Erk, indicating activation of this pathway, the pattern of phospho-Erk staining in KRas tumors was patchy (approximately 30% of the total tumor area), whereas Raf-1 tumors stained more homogeneously throughout (Figure 4A). This again indicates that, whereas Raf-1–Erk signaling cascade contributes to KRas-induced gliomagenesis, it may not be the only critical pathway activated by KRas. In support of this, KRas gliomas also had low but detectable levels of phospho-Akt (Ser473), whereas Raf-1 tumors had no detectable phospho-Akt (Figure 4B). Thus, whereas the KRas– and Raf-1–induced gliomas could be described to be in the same continuum, they were not identical, confirming that although the oncogenic effect of KRas may be transduced largely through Raf-1 signaling in the context of *Arf* loss, other signaling pathways such as PI3K-Akt may also play a role in tumor formation, accounting for the different growth rates of the two tumor types. Both tumors had glial character, as evidenced by GFAP and nestin immunostaining, and were highly proliferative, as shown by PCNA immunohistochemistry (Figure 4, C and D).

## Raf-1 Activation Cooperates with Akt Activation in GBM Formation

We previously demonstrated cooperation between KRas and Akt activation in GBM formation in *Ntv-a wt* mice [10,13,21]. Those tumors were highly similar to human GBMs in that they demonstrated microvascular proliferation, pseudopalisading necrosis, and nuclear atypia—the hallmark features of human GBMs (Figure 5*A*). To investigate whether Raf-1 activation can also cooperate with activation of Akt, we injected *Ntv-a wt* mice with DF1 cells producing RCAS-Raf1 (*n* = 15), or with a combination of DF1 cells producing RCAS-Raf1 and RCAS-Akt (*n* = 25). Whereas Raf-1 alone induced only small hyperplastic lesions in approximately 30% of the mice as discussed in the above paragraphs, a combination of Raf-1 and Akt was able to initiate formation of parenchymal tumors in 52% (13 of 25) of the mice. Of those 13 tumors, 4 presented as small lesions (<5% of the parenchyma), 5 were medium-sized (5% to 30% of the parenchyma), and 3 were large (>30% of the parenchyma) (Figure 5*C*). These tumors had the characteristics of GBMs and were very similar to the KRas+Akt–induced gliomas (Figure 5, *A* and *B*). Immunohistochemical analysis of the tumors showed glial character as indicated by GFAP and nestin staining. They were highly proliferative, as evidenced by PCNA staining. High levels of phospho-Erk indicated an increase in MAPK signaling; phospho-Akt and phospho-S6RP were evidence of increased Akt–mammalian target of rapamycin pathway signaling (Figure 5*B*). Overall, the immunohistochemical features of Raf-1+Akt tumors were similar to both KRas+Akt gliomas and

to human GBMs [10]. These data confirmed cooperation between Raf-1 and Akt activation in glioma formation. Importantly, the tumor latency for the Raf-1+Akt GBMs was longer than that for KRas+Akt tumors [10,18]; this again suggests that, although Raf-MAPK signaling plays an important role in KRas-induced gliomagenesis, this pathway is not solely responsible for tumor formation.

Discussion

Glioblastoma multiforme is a complex disease, with a multitude of genetic aberrations already uncovered, and likely more still to come. In particular, multiple signaling pathways downstream of growth factor receptor tyrosine kinases such as EGFR and PDGFR are upregulated in the majority of GBMs. Therefore, the design of effective mechanism-based drugs depends on the ability to tease apart abnormalities that are causal to tumor formation from those that are secondary events. We previously demonstrated that oncogenic signaling by KRas in cooperation with the loss of *Arf* tumor suppressor or activation of Akt can generate gliomas in mice [8,21,22]. In the present study, we were able to investigate this pathway further and show that, under the same genetic conditions, activated Raf-1 and activated KRas have a similar gliomagenic effect.

Constitutive activation of the RAS-MAPK signaling pathway is a common event in many human cancers that can occur as a result of either abnormal activation of growth factor receptor tyrosine kinases such as EGFR or upregulation of RAS or RAF activity [29]. *BRAF*
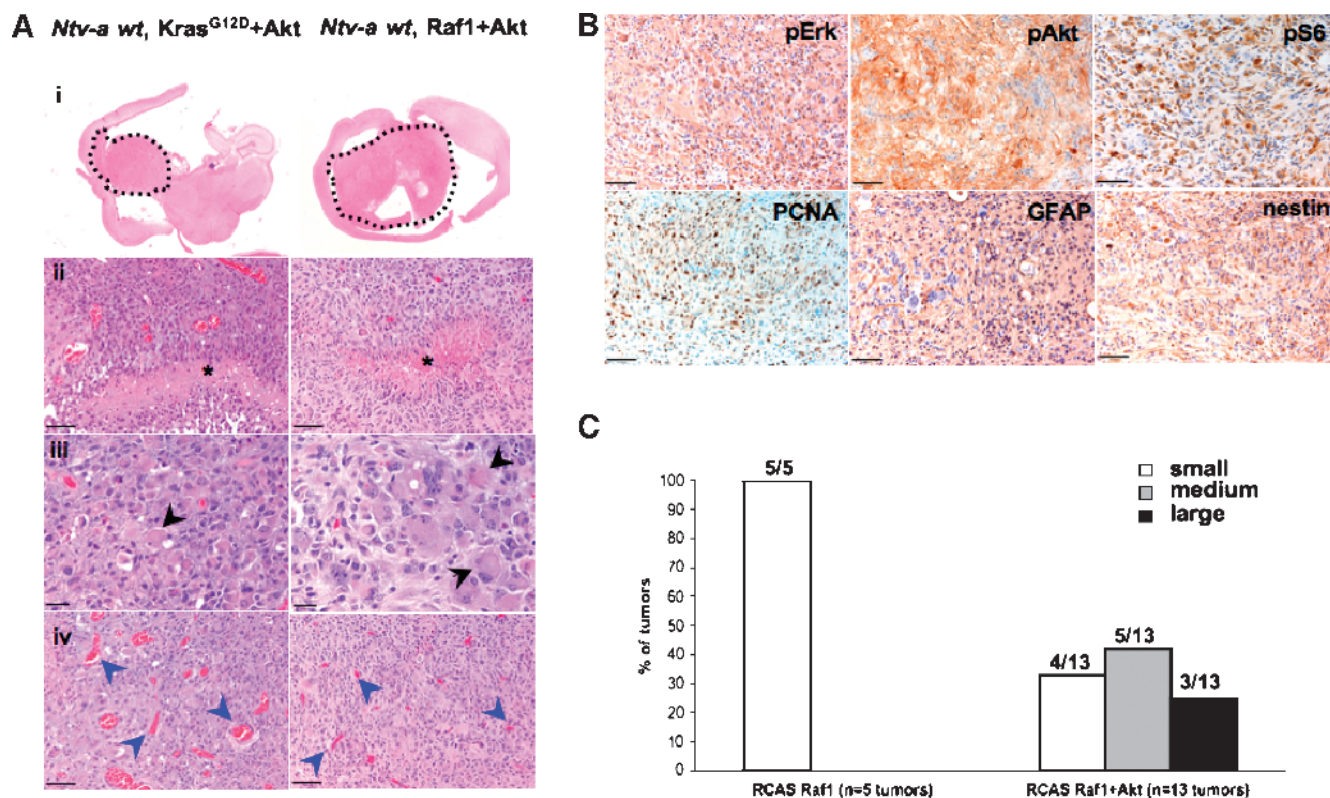
Figure 5. Activated Raf-1 cooperates with activated Akt to induce GBMs in *Ntv-a wt* mice. (A) Histologic comparison of KRas+Akt (left) and Raf-1+Akt GBMs (right). Tumors display the hallmark characteristics of human GBMs: pseudopalisading necrosis (*ii*, asterisks), giant cells (*iii*, black arrowheads), and microvascular proliferation (*iv*, blue arrowheads). Scale bars, 20 (*iii*) and 50 μm (*ii* and *iv*). (B) Representative immunohistochemical analysis of *Ntv-a wt* Raf-1+Akt GBM. Scale bar, 50 μm. (C) Analysis of the tumor size in Raf-1+Akt–driven gliomas (*n* = 13 tumors) compared to Raf-1 alone (*n* = 5 tumors).

mutations have been identified in a variety of cancers, most prominently in melanoma, thyroid, and colorectal tumors [16,19]. Most of those mutations are found in the catalytic domain of the protein and lead to an increase in the kinase activity [30,31]. Interestingly, studies have shown that mutations in *RAS* and *BRAF* are normally mutually exclusive; that is, they do not co-occur in the same tumor [32]. These findings indicate that activation of this pathway is crucially important to the tumor biology and furthermore, that the critical oncogenic effects of RAS are transduced through RAF activity [32,33]. Among the three RAF isoforms (ARAF, BRAF, and CRAF/RAF-1), BRAF has long been considered the one predominantly involved in oncogenic transformation [34,35], mostly because *ARAF* or *RAF-1* mutations had not been found. However, recent studies have identified two separate germ line mutations in *RAF-1* that were associated with a form of acute myeloid leukemia [20]. Additionally, overexpression of RAF-1 has been shown to play a role in pulmonary adenocarcinoma biology [36]. Here, we show that RAF signaling plays an important role in gliomagenesis, despite apparent absence of genetic abnormalities in the *BRAF* and *RAF-1* genes [37,38]. Specifically, Raf-1 activation cooperates with the loss of *Arf* tumor suppressor and/or Akt activation to induce gliomas of varying grades in mice. These findings are significant because these are the genetic alterations frequently seen in human GBMs. Our data are also supported by a finding that a small-molecule inhibitor of RAF was able to block the growth of malignant glioma cell lines *in vitro*, as well as in a xenograft model of glioma [39]. Interestingly, our experiments suggest that tumor initiation and progression may be governed by separate mechanisms, as activated Raf-1 (but not activated KRas) was able to induce small lesions in ~30% of the wild-type mice. Conversely, KRas was more efficient in promoting tumor growth, whereas Raf-induced gliomas had a longer latency in the $Arf^{-/-}$ background. There are several reasons for this phenomenon. One is that other KRas effectors, such as PI3K-Akt, play a role in tumor growth and, because these signals are absent in Raf-1–induced tumors, tumor progression is delayed. Additionally, there may be regulatory mechanisms that govern signal transduction from KRas to Raf-1 that are ineffective when Raf-1 is constitutively activated, thus leading to the formation of hyperplastic lesions. Finally, these studies confirm that activation of the KRas signaling pathway alone is insufficient to initiate malignant glioma formation and requires the presence of other genetic alterations, such as *INK4a-ARF* deficiency. Altogether, these findings have important implications for therapeutic strategies.

Any hope of improving the dismal prognosis of GBM patients is dependent on the ability to correctly identify and target molecular signaling events important for the continued tumor survival and maintenance. Presumably, therapeutics directed against tumor-specific molecular events should achieve that goal while also lessening the general side effects associated with conventional chemotherapy. RAS-MAPK signaling pathway is involved in a multitude of cellular processes, including proliferation, migration, and survival [34,40]. Therefore, taken together with findings by us and by others, it is reasonable to predict that therapeutic inhibition of this pathway might be an effective component in GBM treatment strategy. Currently, there are many compounds targeting the various components of the RAS-MAPK signaling cascade in various phases of clinical trials; those include inhibitors of RAS itself, as well as RAF and MEK inhibitors [34,35,41]. Several of these are also being tested for their efficacy against glioma. Based on the apparent causal role of RAF in gliomagenesis, small-molecule inhibitors of RAF may affect tumor growth. Furthermore, if RAF acts primarily through MEK and MAPK, MEK inhibitors may also be effective. However, two important points must be considered. First, a study examining the sensitivity of melanoma to MEK inhibition determined that only cells harboring a mutation in *BRAF* were susceptible to the drug [42]. It is unknown whether GBMs, which have wild-type *RAF* genes, would respond to this treatment. Secondly, although the MAPK signaling cascade is the most well described pathway of RAF, other MAPK-independent downstream effectors have been implicated in recent years, including components of apoptosis/survival pathways [43,44]. Interestingly, the survival-promoting functions of RAF-1 may not require its kinase activity, with the protein instead acting as a scaffold for other protein assembly [28,44]. Furthermore, there is some evidence of BRAF/RAF-1 heterodimerization, by which BRAF can apparently induce RAF-1 activation; BRAF kinase activity does not appear to be required for this function [40,45]. These mechanisms will be further deciphered through preclinical trials of specific small-molecule inhibitors, elucidating the detailed role of the RAF signaling pathway in GBM biology.

References

[1] Kleihues P, Louis DN, Scheithauer BW, Rorke LB, Reifenberger G, Burger PC, and Cavenee WK (2002). The WHO classification of tumors of the nervous system. *J Neuropathol Exp Neurol* **61**, 215–225 [Discussion 226–219].

[2] Stupp R, Mason WP, van den Bent MJ, Weller M, Fisher B, Taphoorn MJ, Belanger K, Brandes AA, Marosi C, Bogdahn U, et al. (2005). Radiotherapy plus concomitant and adjuvant temozolomide for glioblastoma. *N Engl J Med* **352**, 987–996.

[3] Holland EC (2001). Gliomagenesis: genetic alterations and mouse models. *Nat Rev Genet* **2**, 120–129.

[4] Ichimura K, Bolin MB, Goike HM, Schmidt EE, Moshref A, and Collins VP (2000). Deregulation of the p14ARF/MDM2/p53 pathway is a prerequisite for human astrocytic gliomas with G_1-S transition control gene abnormalities. *Cancer Res* **60**, 417–424.

[5] Ichimura K, Schmidt EE, Goike HM, and Collins VP (1996). Human glioblastomas with no alterations of the *CDKN2A* (p16^INK4a, MTS1) and *CDK4* genes have frequent mutations of the retinoblastoma gene. *Oncogene* **13**, 1065–1072.

[6] Dai C, Celestino JC, Okada Y, Louis DN, Fuller GN, and Holland EC (2001). PDGF autocrine stimulation dedifferentiates cultured astrocytes and induces oligodendrogliomas and oligoastrocytomas from neural progenitors and astrocytes *in vivo*. *Genes Dev* **15**, 1913–1925.

[7] Holland EC, Hively WP, DePinho RA, and Varmus HE (1998). A constitutively active epidermal growth factor receptor cooperates with disruption of G_1 cell-cycle arrest pathways to induce glioma-like lesions in mice. *Genes Dev* **12**, 3675–3685.

[8] Uhrbom L, Kastemar M, Johansson FK, Westermark B, and Holland EC (2005). Cell type–specific tumor suppression by *Ink4a* and *Arf* in Kras-induced mouse gliomagenesis. *Cancer Res* **65**, 2065–2069.

[9] Reilly KM, Loisel DA, Bronson RT, McLaughlin ME, and Jacks T (2000). *Nf1; Trp53* mutant mice develop glioblastoma with evidence of strain-specific effects. *Nat Genet* **26**, 109–113.

[10] Hu X, Pandolfi PP, Li Y, Koutcher JA, Rosenblum M, and Holland EC (2005). mTOR promotes survival and astrocytic characteristics induced by Pten/AKT signaling in glioblastoma. *Neoplasia* **7**, 356–368.

[11] Guha A, Feldkamp MM, Lau N, Boss G, and Pawson A (1997). Proliferation of human malignant astrocytomas is dependent on Ras activation. *Oncogene* **15**, 2755–2765.

[12] Feldkamp MM, Lala P, Lau N, Roncari L, and Guha A (1999). Expression of activated epidermal growth factor receptors, Ras–guanosine triphosphate, and mitogen-activated protein kinase in human glioblastoma multiforme specimens. *Neurosurgery* **45**, 1442–1453.

[13] Rajasekhar VK, Viale A, Socci ND, Wiedmann M, Hu X, and Holland EC (2003). Oncogenic Ras and Akt signaling contribute to glioblastoma formation by differential recruitment of existing mRNAs to polysomes. *Mol Cell* **12**, 889–901.

[14] Ding H, Roncari L, Shannon P, Wu X, Lau N, Karaskova J, Gutmann DH, Squire JA, Nagy A, and Guha A (2001). Astrocyte-specific expression of activated p21–*ras* results in malignant astrocytoma formation in a transgenic mouse model of human gliomas. *Cancer Res* **61**, 3826–3836.

[15] Shannon P, Sabha N, Lau N, Kamnasaran D, Gutmann DH, and Guha A (2005). Pathological and molecular progression of astrocytomas in a GFAP:12 V–Ha-Ras mouse astrocytoma model. *Am J Pathol* **167**, 859–867.

[16] Dhomen N and Marais R (2007). New insight into *BRAF* mutations in cancer. *Curr Opin Genet Dev* **17**, 31–39.

[17] Zebisch A, Czernilofsky AP, Keri G, Smigelskaite J, Sill H, and Troppmair J (2007). Signaling through RAS-RAF-MEK-ERK: from basics to bedside. *Curr Med Chem* **14**, 601–623.

[18] Hindley A and Kolch W (2002). Extracellular signal regulated kinase (ERK)/ mitogen activated protein kinase (MAPK)–independent functions of Raf kinases. *J Cell Sci* **115**, 1575–1581.

[19] Davies H, Bignell GR, Cox C, Stephens P, Edkins S, Clegg S, Teague J, Woffendin H, Garnett MJ, Bottomley W, et al. (2002). Mutations of the *BRAF* gene in human cancer. *Nature* **417**, 949–954.

[20] Zebisch A, Staber PB, Delavar A, Bodner C, Hiden K, Fischereder K, Janakiraman M, Linkesch W, Auner HW, Emberger W, et al. (2006). Two transforming C-RAF germ-line mutations identified in patients with therapy-related acute myeloid leukemia. *Cancer Res* **66**, 3401–3408.

[21] Holland EC, Celestino J, Dai C, Schaefer L, Sawaya RE, and Fuller GN (2000). Combined activation of Ras and Akt in neural progenitors induces glioblastoma formation in mice. *Nat Genet* **25**, 55–57.

[22] Uhrbom L, Dai C, Celestino JC, Rosenblum MK, Fuller GN, and Holland EC (2002). *INK4a-ARF* loss cooperates with KRas activation in astrocytes and neural progenitors to generate glioblastomas of various morphologies depending on activated Akt. *Cancer Res* **62**, 5551–5558.

[23] Stanton VP Jr, Nichols DW, Laudano AP, and Cooper GM (1989). Definition of the human *raf* amino-terminal regulatory region by deletion mutagenesis. *Mol Cell Biol* **9**, 639–647.

[24] Jeuken J, van den Broecke C, Gijsen S, Boots-Sprenger S, and Wesseling P (2007). RAS/RAF pathway activation in gliomas: the result of copy number gains rather than activating mutations. *Acta Neuropathol (Berl)* **114**, 121–133.

[25] Woods SA, Marmor E, Feldkamp M, Lau N, Apicelli AJ, Boss G, Gutmann DH, and Guha A (2002). Aberrant G protein signaling in nervous system tumors. *J Neurosurg* **97**, 627–642.

[26] Uhrbom L and Holland EC (2001). Modeling gliomagenesis with somatic cell gene transfer using retroviral vectors. *J Neurooncol* **53**, 297–305.

[27] Balan V, Leicht DT, Zhu J, Balan K, Kaplun A, Singh-Gupta V, Qin J, Ruan H, Comb MJ, and Tzivion G (2006). Identification of novel *in vivo* Raf-1 phosphorylation sites mediating positive feedback Raf-1 regulation by extracellular signal–regulated kinase. *Mol Biol Cell* **17**, 1141–1153.

[28] Repasky GA, Chenette EJ, and Der CJ (2004). Renewing the conspiracy theory debate: does Raf function alone to mediate Ras oncogenesis? *Trends Cell Biol* **14**, 639–647.

[29] McCubrey JA, Steelman LS, Chappell WH, Abrams SL, Wong EW, Chang F, Lehmann B, Terrian DM, Milella M, Tafuri A, et al. (2007). Roles of the Raf/ MEK/ERK pathway in cell growth, malignant transformation and drug resistance. *Biochim Biophys Acta* **1773**, 1263–1284.

[30] Garnett MJ and Marais R (2004). Guilty as charged: *B-RAF* is a human oncogene. *Cancer Cell* **6**, 313–319.

[31] Wan PT, Garnett MJ, Roe SM, Lee S, Niculescu-Duvaz D, Good VM, Jones CM, Marshall CJ, Springer CJ, Barford D, et al. (2004). Mechanism of activation of the RAF-ERK signaling pathway by oncogenic mutations of *B-RAF*. *Cell* **116**, 855–867.

[32] Kimura ET, Nikiforova MN, Zhu Z, Knauf JA, Nikiforov YE, and Fagin JA (2003). High prevalence of *BRAF* mutations in thyroid cancer: genetic evidence for constitutive activation of the RET/PTC-RAS-BRAF signaling pathway in papillary thyroid carcinoma. *Cancer Res* **63**, 1454–1457.

[33] Yuen ST, Davies H, Chan TL, Ho JW, Bignell GR, Cox C, Stephens P, Edkins S, Tsui WW, Chan AS, et al. (2002). Similarity of the phenotypic patterns associated with *BRAF* and *KRAS* mutations in colorectal neoplasia. *Cancer Res* **62**, 6451–6455.

[34] Roberts PJ and Der CJ (2007). Targeting the Raf-MEK-ERK mitogen-activated protein kinase cascade for the treatment of cancer. *Oncogene* **26**, 3291–3310.

[35] Schreck R and Rapp UR (2006). Raf kinases: oncogenesis and drug discovery. *Int J Cancer* **119**, 2261–2271.

[36] Cekanova M, Majidy M, Masi T, Al-Wadei HA, and Schuller HM (2007). Overexpressed Raf-1 and phosphorylated cyclic adenosine 3′-5′-monophosphatate response element-binding protein are early markers for lung adenocarcinoma. *Cancer* **109**, 1164–1173.

[37] Basto D, Trovisco V, Lopes JM, Martins A, Pardal F, Soares P, and Reis RM (2005). Mutation analysis of *B-RAF* gene in human gliomas. *Acta Neuropathol (Berl)* **109**, 207–210.

[38] Knobbe CB, Reifenberger J, and Reifenberger G (2004). Mutation analysis of the Ras pathway genes *NRAS*, *HRAS*, *KRAS* and *BRAF* in glioblastomas. *Acta Neuropathol (Berl)* **108**, 467–470.

[39] Sathornsumetee S, Hjelmeland AB, Keir ST, McLendon RE, Batt D, Ramsey T, Yusuff N, Rasheed BK, Kieran MW, Laforme A, et al. (2006). AAL881, a novel small molecule inhibitor of RAF and vascular endothelial growth factor receptor activities, blocks the growth of malignant glioma. *Cancer Res* **66**, 8722–8730.

[40] Garnett MJ, Rana S, Paterson H, Barford D, and Marais R (2005). Wild-type and mutant *B-RAF* activate C-RAF through distinct mechanisms involving heterodimerization. *Mol Cell* **20**, 963–969.

[41] Lyustikman Y and Lassman AB (2006). Glioma oncogenesis and animal models of glioma formation. *Hematol Oncol Clin North Am* **20**, 1193–1214.

[42] Solit DB, Garraway LA, Pratilas CA, Sawai A, Getz G, Basso A, Ye Q, Lobo JM, She Y, Osman I, et al. (2006). *BRAF* mutation predicts sensitivity to MEK inhibition. *Nature* **439**, 358–362.

[43] Dhillon AS, Meikle S, Peyssonnaux C, Grindlay J, Kaiser C, Steen H, Shaw PE, Mischak H, Eychene A, and Kolch W (2003). A *Raf-1* mutant that dissociates MEK/extracellular signal–regulated kinase activation from malignant transformation and differentiation but not proliferation. *Mol Cell Biol* **23**, 1983–1993.

[44] Gollob JA, Wilhelm S, Carter C, and Kelley SL (2006). Role of Raf kinase in cancer: therapeutic potential of targeting the Raf/MEK/ERK signal transduction pathway. *Semin Oncol* **33**, 392–406.

[45] Rushworth LK, Hindley AD, O'Neill E, and Kolch W (2006). Regulation and role of Raf-1/B-Raf heterodimerization. *Mol Cell Biol* **26**, 2262–2272.